

# ECOLOGY LETTERS

## Climate drives community-wide divergence within species over a limited spatial scale: Evidence from an oceanic island

Journal:	<i>Ecology Letters</i>
Manuscript ID	ELE-00526-2019.R2
Manuscript Type:	Letters
Date Submitted by the Author:	16-Sep-2019
Complete List of Authors:	<p>Salces-Castellano, Antonia ; IPNA-CSIC, Island Ecology and Evolution Research Group  Patiño, Jairo; Instituto de Productos Naturales y Agrobiología, Island Ecology and Evolution Research Group  Alvarez, Nadir; Natural History Museum of Geneva, N/A  Andújar, Carmelo; IPNA-CSIC, Island Ecology and Evolution Research Group  Arribas, Paula; IPNA-CSIC, Island Ecology and Evolution Research Group  Braojos-Ruiz, Juan José; Tenerife Insular Water Council , N/A  del Arco, Marcelino; Universidad de La Laguna, Departamento de Botánica, Ecología y Fisiología Vegetal  García-Olivares, Víctor; IPNA-CSIC, Island Ecology and Evolution Research Group  Karger, Dirk Nikolaus; University of Zurich, Institute of Systematik Botany  López, Heriberto; IPNA-CSIC, Island Ecology and Evolution Research Group  Manolopoulou, Ioanna; University College London, Department of Statistical Science  Oromí, Pedro; University of La Laguna, Department of Animal Biology  Pérez-Delgado, Antonio; IPNA-CSIC , Island Ecology and Evolution Research Group  Peterman, William ; Ohio State University, Environment and Natural Resources  Rijdsdijk, Kenneth; University of Amsterdam, Institute for Biodiversity and Ecosystem Dynamics  Emerson, Brent; IPNA-CSIC, Island Ecology and Evolution Research Group</p>

**Letter****Climate drives community-wide divergence within species over a limited spatial scale:  
Evidence from an oceanic island**

Antonia Salces-Castellano<sup>1,2†</sup>, Jairo Patiño<sup>1,3†</sup>, Nadir Alvarez<sup>4</sup>, Carmelo Andújar<sup>1</sup>, Paula Arribas<sup>1</sup>, Juan José Braojos-Ruiz<sup>5</sup>, Marcelino del Arco-Aguilar<sup>3</sup>, Víctor García-Olivares<sup>1,2</sup>, Dirk Karger<sup>6</sup>, Heriberto López<sup>1</sup>, Ioanna Manolopoulou<sup>7</sup>, Pedro Oromí<sup>8</sup>, Antonio J. Pérez-Delgado<sup>1,2</sup>, William E. Peterman<sup>9</sup>, Kenneth F. Rijdsdijk<sup>10</sup>, & Brent C. Emerson<sup>1\*</sup>

1. Island Ecology and Evolution Research Group, Institute of Natural Products and Agrobiology (IPNA-CSIC), C/Astrofísico Francisco Sánchez 3, La Laguna, Tenerife, Canary Islands, 38206, Spain
2. School of Doctoral and Postgraduate Studies, University of La Laguna, 38200, La Laguna, Tenerife, Canary Islands, Spain
3. Plant Conservation and Biogeography Group, Department of Botany, Ecology and Plant Physiology, University of La Laguna, C/ Astrofísico Francisco Sánchez, 38206 La Laguna, Tenerife, Canary Islands, Spain.
4. Natural History Museum of Geneva, 1 route de Malagnou, 1208 Geneva, Switzerland.
5. Tenerife Insular Water Council (CIATF), C/ Leoncio Rodríguez 2, 38003, Santa Cruz de Tenerife, Spain.
6. Swiss Federal Research Institute WSL, Züricherstrasse 111, 8903 Birmensdorf, Switzerland
7. Department of Statistical Science, University College London, London, United Kingdom.
8. Department of Animal Biology, Edaphology and Geology, University of Laguna, C/ Astrofísico Francisco Sánchez, 38206 La Laguna, Tenerife, Canary Islands, Spain.
9. School of Environmental and Natural Resources, The Ohio State University, Columbus, OH, USA.
10. Institute for Biodiversity and Ecosystem Dynamics, University of Amsterdam, Amsterdam, Netherlands.

† These authors contributed equally

\* Corresponding author: bemerson@ipna.csic.es, ph: +34 922 256 847

Key words: climate, topography, dispersal, gene flow, Quaternary, arthropod, beetle, speciation

**Running title.** Climate drives community-wide diversification

**Author contributions.** B.C.E. designed and coordinated the study. A.J.P.-D., H.L., P.O. and B.C.E. did the field work. A.J.P.-D led sample sorting with input from H.L., A.S.-C. and P.O. H.L. and A.S.-C generated the mtDNA sequence data. J.P. and V.G.-O. generated the ddRAD-seq data. D.K. generated the topoclimatic data, with input from J.P. A.S.-C. led the mtDNA analyses with input from

1  
2  
3  
4  
5  
6  
7  
8  
9  
10 B.C.E., J.P., I.M., P.A. and C.A. J.P. led ddRAD-seq data analyses, with input from B.C.E. and N.A.  
11 J.P. conducted ResistanceGA analyses, with input from W.E.P. M.J.d.A.-A., J.J.B.-J. and K.R.  
12 contributed local floristic, climate and geological expertise, respectively. B.C.E., A.S.-C. and J.P.  
13 wrote the manuscript, with contributions from all authors.  
14  
15

16 **Data availability.** Mitochondrial sequence data, filtered SNP data and topoclimate data are available  
17 from the Dryad Digital Repository [https://doi.org/\[to be made available upon acceptance\]](https://doi.org/[to be made available upon acceptance]). Raw  
18 demultiplexed sequences for the full ddRAD-seq data set are available on NCBI SRA (BioProject  
19 Accession [to be made available upon acceptance]).  
20  
21

22 Abstract word count: 152  
23 Main text word count: 5000  
24 Number of references: 65  
25 Number of figures: 4  
26 Number of tables: 0  
27  
28  
29  
30  
31  
32  
33  
34  
35  
36  
37  
38  
39  
40  
41  
42  
43  
44  
45  
46  
47  
48  
49  
50  
51  
52  
53  
54  
55  
56  
57  
58  
59  
60

**Abstract**

Geographic isolation substantially contributes to species endemism on oceanic islands when speciation involves the colonisation of a new island. However, less is understood about the drivers of speciation within islands. What is lacking is a general understanding of the geographic scale of gene flow limitation within islands, and thus the spatial scale and drivers of geographical speciation within insular contexts. Using a community of beetle species, we show that when dispersal ability and climate tolerance are restricted, microclimatic variation over distances of only a few kilometres can maintain strong geographic isolation extending back several millions of years. Further to this, we demonstrate congruent diversification with gene flow across species, mediated by Quaternary climate oscillations that have facilitated a dynamic of isolation and secondary contact. The unprecedented scale of parallel species responses to a common environmental driver for evolutionary change has profound consequences for understanding past and future species responses to climate variation.

## INTRODUCTION

Islands are often viewed as theatres for adaptive evolutionary change and speciation (Losos & Ricklefs 2009), where non-adaptive paths to speciation are frequently given limited importance, or even ignored (e.g. Cabral *et al.* 2019). Recent models have sought to understand how geophysical island attributes influence insular biodiversity through the regulation of colonisation, speciation and extinction (e.g. Whittaker *et al.* 2008; Fernández-Palacios *et al.* 2016; Lim & Marshall 2017). Although such models have sought to account for both long-term island ontogeny (e.g. Whittaker *et al.* 2008; Borregaard *et al.* 2017) and shorter-term surface area changes (e.g. Fernández-Palacios *et al.* 2016; Weigelt *et al.* 2016), insular species themselves have received much less attention (but see Rosindell & Harmon 2013; Rominger *et al.* 2016; Cabral *et al.* 2019 for models incorporating species properties and biotic interactions). While much quantitative molecular data exists on insular speciation across archipelagos (e.g. Shaw & Gillespie 2016), it is difficult to compare across such studies and generalise about the drivers of speciation within islands. This is because independent studies are idiosyncratic with regard to geographic sampling, and tend to be taxonomically biased toward diversified lineages. More importantly, such studies are largely focussed on describing patterns of speciation rather than the underlying processes that give rise to speciation. Despite these limitations, support has been found for a model where there is a significant correlation between the spatial scales of gene flow and speciation (Kisel & Barraclough 2010). However, the importance and mechanistic basis of non-adaptive evolutionary pathways to speciation, where physical disruption of gene flow initiates divergence and ultimately promotes speciation, remains poorly understood.

Goodman *et al.* (2012) have noted that relatively rapid geological events within islands may be important drivers of divergence and speciation, and several studies implicate the fragmenting actions of volcanic activity (e.g. Vandergast *et al.* 2004) and flank collapses (e.g. Brown *et al.* 2006) as dispersal barriers. However, little attention has been focussed on the potential for local climate variation to act as a barrier to dispersal. Recently, García-Olivares *et al.* (2019) have proposed an

1  
2  
3  
4  
5  
6  
7  
8  
9  
10 insular topographic Quaternary diversification (ITQD) model, whereby genetic variation is structured  
11 by the geography of suitable climate. They used nuclear genomic data for a species complex of  
12 weevils (*Laparocerus tessellatus*) on the island of Gran Canaria (Canary Islands) to present evidence  
13 for geographic variation in humidity structuring genetic variation. Further to this, their results  
14 supported the influence of Quaternary climatic oscillations on contemporary patterns of genomic  
15 relatedness among individuals.  
16  
17  
18  
19

20 The results of García-Olivares *et al.* (2019) suggest a potentially important role for climate as  
21 a driver of population isolation and differentiation within islands, as landscape discontinuities for  
22 climate may similarly impact all species co-occurring in a given territory. Here we use laurel forest  
23 beetle species to test the hypothesis that fine-scale spatial variation in microclimate can disrupt gene  
24 flow and structure genetic variation in a concerted manner across species. Laurel forests occur in  
25 areas of high humidity, and are the ecosystem characterised by the highest levels of arthropod  
26 diversity within Macaronesia, of which many species are hydrophilic and restricted to this ecosystem  
27 (Fernández-Palacios *et al.* 2017). Both humidity and temperature are known to vary geographically  
28 within laurel forests (Braojos Ruiz 2015), providing the potential for geographic structuring of genetic  
29 variation within species. If landscape variation in humidity and temperature results in unfavourable  
30 areas for individual survival and/or establishment, then areas of favourable environmental conditions  
31 will be isolated if species are unable to disperse across unfavourable areas.  
32  
33  
34  
35  
36  
37  
38  
39

40 We focus our sampling within the laurel forest of the Anaga peninsula on the Canary Island  
41 of Tenerife, as the recent geological history of Anaga is one of relative stability. Anaga began to grow  
42 in the late Miocene, with the last major period of its polygenetic evolution about 4.2 Ma (million  
43 years ago) (Thirlwall *et al.* 2000), with relative quiescence from around 3.3 Ma (Ancochea *et al.*  
44 1990). The absence of younger volcanoclastics on Anaga indicate minimal impact from intense  
45 volcanic activity over the last several million years in the centre and south of the island (Carracedo  
46 2011). Additionally, while most of the northern flank of Tenerife has suffered catastrophic flank  
47 collapses, some as recently as 150 Ka (thousand years ago) (García-Olivares *et al.* 2017), only one  
48  
49  
50  
51  
52  
53  
54  
55  
56  
57  
58  
59  
60

1  
2  
3  
4  
5  
6  
7  
8  
9  
10 such flank collapse is known for the Anaga Peninsula, estimated to have occurred 4.1 - 4.7 Ma (Walter  
11 *et al.* 2005). Thus, the Anaga peninsula represents a relatively geologically stable region, where  
12 millennial-scale erosional activity and climate variation have been more consequential than  
13 catastrophic geological events, at least over the last 3 Ma. This provides a near ideal template within  
14 which to assess how landscape discontinuities for suitable environmental conditions impact upon  
15 spatial patterns of genetic relatedness within species.  
16  
17  
18  
19

20 We first generated six climatic and topographical layers that are expected to have some  
21 functional relationship to water stress or geographical isolation across the dorsal ridge that runs east-  
22 west along the Anaga peninsula (Fig. 1), at a resolution of 90 m<sup>2</sup>. Within this area we then used an  
23 intensive sampling protocol (Emerson *et al.* 2017) to sample Coleoptera from ten 50m x 50m plots  
24 within the laurel forest of the peninsula, which were then classified to presumed biological species  
25 (PBS) using a modification of the protocol of Emerson *et al.* (2017). Mitochondrial DNA was used  
26 to generate estimates of population genetic structure among sampling sites within each PBS, and  
27 these individual estimates were then summarised as pairwise dissimilarity among sampling sites  
28 across all PBS. For comparative purposes, two pairwise beta diversity matrices were also calculated,  
29 one using PBS distribution data, and one using individual haplotypes. The five community-level  
30 dissimilarity matrices were then used to assess patterns of geographic structure and to test between  
31 hypotheses of isolation by distance, or isolation by unfavourable areas of higher water stress that limit  
32 gene flow in species with high humidity requirements. We then tested species-specific predictions  
33 derived from these results using genomic datasets obtained from double-digest restriction site-  
34 associated DNA sequencing (ddRAD-seq) for 16 PBS.  
35  
36  
37  
38  
39  
40  
41  
42  
43  
44  
45  
46

## 47 **MATERIALS AND METHODS**

### 48 **Sampling, specimen sorting into parataxonomic units and mtDNA sequencing**

49  
50  
51  
52  
53  
54  
55  
56  
57  
58  
59  
60

1  
2  
3  
4  
5  
6  
7  
8  
9  
10 Ten sampling plots of 50m x 50m were established within the laurel forest of the Anaga peninsula,  
11 on the island of Tenerife in the Canary Islands (Fig. 1, see Appendix S1 for further details). A  
12 standardised sampling protocol (Emerson *et al.* 2017) was applied to each plot, with sampling  
13 undertaken between Nov 2012 and April 2013. Specimen sorting into parataxonomic units (PUs)  
14 was conducted using the protocol of Emerson *et al.* (2017), with minor modifications (see Appendix  
15 S1). Within each plot, four individuals from each sampled PU (less if fewer than four were sampled)  
16 were sequenced for a 824 bp region of the mtDNA COI gene (see Appendix S1 for details).  
17  
18  
19  
20  
21  
22

### 23 **Delimitation of presumed biological species and taxonomic assignment**

24  
25 We used a modification of Emerson *et al.* (2017) for the inference of PBS (see Appendix S1 for  
26 details). Final taxonomic assignment for PBS was made using the taxonomic literature and a  
27 reference collection of Canary Island beetles maintained by one of us (PO). For taxonomically  
28 complex groups for which a molecular phylogeny is available (e.g. Cryptorhynchinae (Stüben &  
29 Astrin 2010), *Laparocerus* (Machado *et al.* 2017)), final taxonomic assignment was aided by  
30 phylogenetic assignment after sequencing several individuals of a PBS for a corresponding gene  
31 region.  
32  
33  
34  
35  
36  
37  
38

### 39 **Bayesian inference of phylogeographic clusters**

40 We used the R package BPEC (Bayesian Phylogeographic and Ecological Clustering)  
41 (Manolopoulou *et al.* 2011) to identify genetically distinct geographical population clusters within  
42 each PBS. The program used a fully model-based framework to generate posterior probabilities for  
43 phylogeographic groupings, combining a parsimony-based evolutionary model for genealogical  
44 relationships among DNA sequences, together with a geographical model representing dispersal  
45 events consistent with geographically coherent clusters of related sequences. The following  
46 parameters were chosen to achieve convergence: (i) maximum number of migrations (maxMig =  
47 5), (ii) parsimony relaxation parameter (ds = 0), and (iii) number of iterations (iter = 10,000,000).  
48  
49  
50  
51  
52  
53  
54  
55  
56  
57  
58  
59  
60



1  
2  
3  
4  
5  
6  
7  
8  
9  
10 For each PBS a MCMC sampler was run to obtain phylogeographic clusters. Results for each PBS  
11 were then summarised within a pairwise matrix of locations where: 1 = both locations were sampled  
12 for the same phylogroup, 0 = each location was sampled for a different phylogroup, NA = one or  
13 both locations were not sampled. Results across all matrices were integrated to create a single matrix  
14 where each cell represents the proportion of PBS sampled from a pair of locations that belong to the  
15 same phylogroup.  
16  
17  
18  
19

### 20 21 **PBS and intraspecific mtDNA beta diversity and dissimilarity**

22  
23 A pairwise beta diversity matrix, including beta components [i.e.  $\beta_{\text{Sorensen}}$ ,  $\beta_{\text{Simpson}}$  and  $\beta_{\text{nestedness}}$ ] were  
24 calculated among all plots at the level of PBS using the R package betapart (Baselga & Orme 2012).  
25 Pairwise dissimilarity of assemblages among sites was also assessed at the intraspecific level. First,  
26 we generated a pairwise beta diversity matrix at the haplotype level using the same approach as that  
27 for PBS, but in this case based on the presence/absence of haplotypes across all plots (Baselga *et al.*  
28 2013). In this analysis all haplotypes from all PBS are used in a single analysis. Second, we assessed  
29 dissimilarity at the intraspecific level using (i)  $G_{\text{ST}}$  to partition haplotype variation within PBS and  
30 (ii)  $N_{\text{ST}}$  to also account for haplotype relatedness. For each PBS, total and pairwise  $G_{\text{ST}}$  and  $N_{\text{ST}}$   
31 among plots were estimated using SPAGeDi (Hardy & Vekemans 2002), and pairwise values were  
32 then used to calculate average  $G_{\text{ST}}$  and  $N_{\text{ST}}$  for all pairs of plots using all PBS, providing novel  
33 pairwise dissimilarity matrices at the intraspecific level.  
34  
35  
36  
37  
38  
39  
40  
41  
42  
43

### 44 **Hierarchical cluster analyses and homogeneity analyses**

45 The five dissimilarity matrices described above (PBS, phylogroup,  $G_{\text{ST}}$ ,  $N_{\text{ST}}$ , and haplotype) were  
46 used to perform hierarchical cluster analysis using Ward's agglomerative method (Murtagh &  
47 Legendre 2014). To identify the more strongly differentiated and internally homogenous groups of  
48 plots based on dissimilarity matrices, homogeneity analyses were performed to assess the increase  
49 in the average within-group pairwise similarity across the groups defined by the corresponding  
50  
51  
52  
53  
54  
55  
56  
57  
58  
59  
60

1  
2  
3  
4  
5  
6  
7  
8  
9  
10 hierarchical classification (Bedward *et al.* 1992). Permutational ANOVAs (Permanova) were  
11 conducted to test for significant differences across the defined groups of plots for each of the five  
12 dissimilarity matrices.  
13  
14  
15

#### 16 **MtDNA network analyses and estimation of divergence times**

17  
18 MtDNA haplotype networks for 15 PBS and a sister PBS pair selected for ddRAD-seq (see next  
19 section) were constructed in SplitsTree v.4.14.6 (Huson & Bryant 2006), using the NeighborNet  
20 method with K2P distances. Divergence times were estimated with BEAST v.2.5.0 (Bouckaert *et*  
21 *al.* 2014), applying: (i) optimal models for each alignment inferred with jModeltest2 (Darriba *et al.*  
22 2012) (Table S1); (ii) a strict clock, which is frequently used in analyses of sequence data sampled  
23 at the intraspecific level (Ho & Duchêne 2014), for which the use of the relaxed molecular clock is  
24 not appropriate (Hein *et al.* 2005); (iii) a constant size coalescent prior, and; (iv), a uniform prior  
25 distribution representing the 95% confidence interval around a beetle specific rate estimate of  
26 0.0177 ( $\pm$  0.0038) for the mtDNA COI gene (Papadopoulou *et al.* 2010). MCMC analyses were run  
27 for 100,000,000 steps, sampling every 1,000 steps, with the first 10% discarded as burnin, using  
28 values of effective samples size (ESS) greater than 200 as a minimum for acceptance.  
29  
30  
31  
32  
33  
34  
35  
36  
37  
38

#### 39 **Double-digest restriction site-associated DNA sequencing and de novo assembly**

40  
41 Based on inferences from community-level analyses, 15 PBS and a sister PBS pair were selected  
42 for double-digest restriction site-associated DNA sequencing (ddRAD-seq). ddRAD-seq libraries  
43 were prepared following the protocol of García-Olivares *et al.* (2019) with some minor  
44 modifications (see results). ddRAD-seq libraries for each PBS were processed using the iPyrad  
45 v0.7.19 pipeline (<http://ipyrad.readthedocs.io/>). De novo assembly details can be found in Appendix  
46 S1.  
47  
48  
49  
50  
51

#### 52 **Genomic population structure and differentiation**

1  
2  
3  
4  
5  
6  
7  
8  
9  
10 To explore population structure within each of the 16 ddRAD-seq datasets, we first constructed  
11 phylogenetic networks, using the NeighborNet algorithm implemented in SplitsTree 4 (Huson &  
12 Bryant 2006). Principal component analyses (PCA) were performed with the R package adegenet  
13 v. 2.1.1 (Jombart & Ahmed 2011). To explore population genetic structure across sampling sites,  
14 we used a model-based clustering analysis that estimates individual ancestry coefficients  
15 representing the proportions of an individual genome that originate from multiple ancestral gene  
16 pools. Calculations were implemented in the program sNMF based on sparse non-negative matrix  
17 factorization and least-squares optimization (Frichot *et al.* 2014). Ancestry coefficients estimated  
18 using the sNMF method have been shown to produce results that are comparable to other widely  
19 used programs such as ADMIXTURE and STRUCTURE, but have the advantage of estimating  
20 homozygote and heterozygote frequencies and avoiding Hardy-Weinberg equilibrium assumptions  
21 (Frichot *et al.* 2014). We calculated ancestry coefficients for 1-10 ancestral populations (K) using  
22 10 replicates for each K. We used a cross-entropy criterion, based on the prediction of masked  
23 genotypes to evaluate the error of ancestry estimation, to identify optimal values for K. The sNMF  
24 method was implemented in the R package LEA (Frichot *et al.* 2015).

### 35 36 **Climate modelling and environmental layers**

37 We modelled mean annual temperature (TEMP) and mean annual precipitation (PREC) using  
38 geographically weighted regression (GWR) with station data from the Spanish Agency of  
39 Meteorology ([www.aemet.es](http://www.aemet.es)). We used 152 stations and 217 stations for temperature and  
40 precipitation, respectively. A digital elevation model (DEM) at a resolution of ~90m<sup>2</sup> resolution was  
41 derived from CGIAR-CSI SRTM v4.1 and ASTER GDEM v2 data products (Robinson *et al.* 2014).  
42 For temperature we calculated a GWR with elevation (ELEV) of the DEM as a predictor variable  
43 and a Gaussian kernel. For precipitation we also used a GWR with a Gaussian kernel, using the  
44 windward / leeward index (Böhner & Antonic 2008; Karger *et al.* 2017), and elevation as predictors.  
45 We additionally applied a residual interpolation using the station data to remove uncertainties in  
46  
47  
48  
49  
50  
51  
52  
53  
54  
55  
56  
57  
58  
59  
60

1  
2  
3  
4  
5  
6  
7  
8  
9  
10 temperature and precipitation not captured by the GWR. The residuals were then interpolated using  
11 a multilevel B-spline interpolation with fourteen error levels. The resulting layers were then added  
12 to the GWR predictions in order to obtain the final temperature and precipitation layers. For  
13 topographic wetness (WET) we used the SAGA wetness index (Böhner & Antonic 2008) in SAGA  
14 GIS Vers. 6.0.0 (Conrad *et al.* 2015), in order to describe the tendency of a cell to accumulate water.  
15 Finally, from the ELEV layer in SAGA QGIS, two additional topographic indices of position (POS)  
16 and ruggedness (RUG) were estimated.  
17  
18  
19  
20  
21  
22

### 23 **Landscape resistance analyses**

24  
25 We used the R package ResistanceGA v. 4.0 (Peterman 2018) to assess the effects of the landscape  
26 factors described above (TEMP, PREC, ELEV, WET, POS, RUG) on connectivity among sampling  
27 plots. Using a genetic algorithm and mixed effects models fit based on the maximum-likelihood  
28 population effects parameterization (Clarke *et al.* 2002), this method optimizes resistance surface  
29 values such that effective distances between sample locations across the landscape best fit the  
30 observed genetic differentiation or community dissimilarity between locations. ResistanceGA is  
31 unique among available approaches for landscape resistance modelling in that it is a true optimization  
32 of landscape resistance values, avoiding subjectivity in assigning resistance values (Peterman *et al.*  
33 2014; Peterman 2018).  
34  
35  
36  
37  
38  
39

40 We assessed the effects of the different landscape factors on multiple different pairwise  
41 distance measures. These distance measures were estimated at the level of sampling sites (i.e.  
42 community-level data) or individuals, as follows: (i) for the community-level matrices, we used the  
43 five dissimilarity matrices described above (i.e. PBS, phylogroup,  $G_{ST}$ ,  $N_{ST}$ , and haplotype); and (ii)  
44 for individuals within each of the 16 ddRAD-seq data sets, we followed the approach proposed by  
45 Petkova *et al.* (2015). Effective distances between sample sites were calculated as the random-walk  
46 commute time (van Etten 2017), which is a multi-path distance measure equivalent to resistance  
47 distance (Kivimäki *et al.* 2014), as calculated by CIRCUITSCAPE (McRae *et al.* 2008; McRae &  
48  
49  
50  
51  
52  
53  
54  
55  
56  
57  
58  
59  
60

1  
2  
3  
4  
5  
6  
7  
8  
9  
10 Shah 2009). We used the “all\_comb” function in ResistanceGA to optimize all single- and multiple-  
11 surface combinations of resistance surfaces (up to three surfaces within a model). For multiple-  
12 surface optimization, resistance surfaces were combined during optimization to create novel  
13 composite resistance surfaces. We used AICc to assess support for optimized resistance surfaces,  
14 and fitted mixed effects models with a  $\Delta AICc < 2$  were deemed to be equally supported.  
15  
16  
17  
18

## 19 **RESULTS**

### 20 **Sampling and delimitation of presumed biological species**

21  
22  
23  
24  
25 A total of 23,180 Coleoptera specimens were sampled across the 10 plots, from which a total of 2,181  
26 individuals were selected for DNA sequencing based on initial assignment to PUs, of which 1,919  
27 were successfully amplified and sequenced. Two PUs, corresponding to the taxonomic species  
28 *Tarphius canariensis* and *T. simplex* were removed from subsequent analysis as they did not segregate  
29 based on mtDNA, consistent with previous suggestions of incomplete lineage sorting within this  
30 group (Emerson *et al.* 2000), or hybridisation. A total of 154 PBS were identified, of which 146 are  
31 identified as native or endemic to the Canary Islands, yielding a total of 1786 mtDNA sequences  
32 corresponding to 950 different haplotypes.  
33  
34  
35  
36  
37  
38  
39

### 40 **Community-level geographic structuring of genetic variation within species**

41  
42 A consistent community-level signal for the structuring of intraspecific genetic variation into two  
43 regions was observed, hereafter referred to as East and West (Fig. 2). This contrasts with the pattern  
44 observed when dissimilarity was measured at the level of PBS. The intraspecific signature was  
45 strongest when phylogeographic groupings within PBS were considered, with the Permanova  
46 analysis revealing that 78% of dissimilarity among sampling plots was explained by phylogeographic  
47 differences between East and West. A more limited signal was recovered when intraspecific genetic  
48 variation was summarised as  $N_{ST}$  and  $G_{ST}$  (Permanova  $R^2 = 0.44$  and  $0.38$  respectively), while  
49  
50  
51  
52  
53  
54  
55  
56  
57  
58  
59  
60

1  
2  
3  
4  
5  
6  
7  
8  
9  
10  
11  
12  
13  
14  
15  
16  
17  
18  
19  
20  
21  
22  
23  
24  
25  
26  
27  
28  
29  
30  
31  
32  
33  
34  
35  
36  
37  
38  
39  
40  
41  
42  
43  
44  
45  
46  
47  
48  
49  
50  
51  
52  
53  
54  
55  
56  
57  
58  
59  
60

dissimilarity of haplotypes between East and West only explained 11% of the variation among sampling plots. Resistance landscape analyses of the six topoclimatic variables (Fig. 2c) revealed that patterns of community dissimilarity are best explained as a function of geographic distance when intraspecific variation is summarised with  $N_{ST}$  and  $G_{ST}$ . When considering all haplotypes across all PBS, both temperature and geographic distance best explained variation in community similarity. When considering dissimilarity in PBS composition, both topographic wetness and geographic distance best explained dissimilarity among communities. However, when intraspecific variation was partitioned into phylogroups, landscape variation in mean annual precipitation alone followed by elevation best explained community dissimilarity.

#### Sequencing and de novo assembly of ddRAD-seq data

Seven PBS and a sister PBS pair were chosen to represent East-West structuring of mtDNA variation consistent with community-level patterns detected with the above-described analyses of mtDNA variation. Selected PBS presented East-West structure based on BPEC analyses together with significantly positive values for both  $G_{ST}$  and  $N_{ST}$ . The sister PBS pair comprised two previously described mtDNA lineages (Schütte & Stüben 2015) that assign unambiguously to *Acalles globulipennis*, with a divergence marginally exceeding our conservative 8% Kimura two-parameter threshold between species (see Methods and Appendix S1). Nuclear genomic data for these two PBS revealed congruent differentiation, but also evidence for incomplete reproductive isolation (see Results). For simplicity, we hereafter refer to all individuals of *A. globulipennis* as one PBS, while recognising it to be more consistent with a species complex.

A total of 235 individuals were selected for analysis, for an average of  $14.7 \pm 5.4$  (9-26) individuals per PBS (Table S2). A minimum level of DNA sample concentration ( $> 0.5$  ng/ $\mu$ l) was achieved for all samples, with an average concentration of  $22.8 \pm 4.0$  ng/ $\mu$ l. A total of four libraries were prepared, randomly selecting four PBS for each library and including a randomly-selected replicate per PBS and a blank control per library. On the basis of fragment spectrums measured for

1  
2  
3  
4  
5  
6  
7  
8  
9  
10 each of the 16 PBS prior to pooling using a Fragment Analyzer (Advanced Analytical), libraries  
11 were then size selected between 225 bp and 275 bp using the Pippin Prep electrophoresis platform  
12 (Sage Science) and fragment spectrums for each pool were then verified with a Fragment Analyzer.  
13 All libraries were pooled and sequenced on four lanes of Illumina HiSeq2500 using the single-end  
14 (100 bp) protocol at the Lausanne Genomic Technologies Facility. Twenty-three samples did not  
15 sequence well and were removed from further analyses. The 16 ddRAD-seq libraries yielded an  
16 average of 44,685,100 raw reads (S.D. = 7,104,526). Depending on the PBS, we recovered between  
17 2,775 and 34,339 loci, including from 2,663 to 33,835 unlinked biallelic SNPs, with between 0.9 to  
18 7.19% missing data (Table S2).  
19  
20  
21  
22  
23  
24  
25

#### 26 **Species-specific testing of predictions from community-level inference**

27  
28 Among the eight PBS with strong regional structuring of mtDNA variation, estimates for the onset  
29 of regional divergence ranged from 0.5 Ma (*Rhopalomesites persimilis*, 95% HPD: 0.2-0.8 Ma) to  
30 4.6 Ma (*Acalles globulipennis*, 95% HPD: 2.5-7 Ma) (Table S1). For all PBS, minimum spanning  
31 networks, principal component analyses and model-based ancestry estimation revealed three  
32 consistent features: (i) East-West structuring of nuclear genetic variation; (ii) evidence for ancestral  
33 populations consistent with East and West; and (iii) signatures of localised admixture among  
34 populations, frequently involving sites five and six, but in some cases extending to adjacent sites,  
35 with the exception of a single PBS not sampled at sites five and six (Fig. 3 and Fig. S1). Landscape  
36 resistance analyses revealed that patterns of genomic relatedness among individuals within all eight  
37 PBS are best explained by one or more climatic or topographical variables (Fig. S1 and Table S3).  
38  
39  
40  
41  
42  
43  
44  
45 Geographic distance did not feature in the set of best supported models for any of the eight PBS.

46  
47 Among the eight PBS presenting no evidence for regional structuring of mtDNA variation,  
48 three presented only limited signatures for geographic structure of nuclear genetic variation, with  
49 individual relatedness best explained by geographic distance, or the null model (Fig. S1). However,  
50 for the remaining five PBS, ddRAD-seq data revealed the same three features of (i) East-West  
51  
52  
53  
54  
55  
56  
57  
58  
59  
60

1  
2  
3  
4  
5  
6  
7  
8  
9  
10 separation, (ii) ancestral assignment to the East and West populations, and (iii) admixture centred  
11 around sites five and six. Additionally, genomic relatedness among individuals for all five PBS is  
12 best explained by climatic or topographical variables (Fig. S1). Maximum age estimates for the onset  
13 of regional divergence within these five PBS ranged from 0.1 Ma (95% HPD: 0-0.2 Ma) to 0.9 Ma  
14 (95% HPD: 0.4-1.4 Ma) (Table S1).  
15  
16  
17  
18

## 19 **DISCUSSION**

20  
21  
22  
23 Strong support was found for community-level structuring of genetic variation between East and  
24 West when considering phylogeographic structure within PBS, with landscape variation for elevation  
25 and precipitation best explaining this structure (Fig. 2). The lack of similarly high support from other  
26 measures of intraspecific dissimilarity can be reconciled with the differing impact of unstructured  
27 PBS among the different analyses. Information content for the phylogeographic analysis is restricted  
28 to the 36 PBS that presented more than one phylogroup, while all PBS contributed to dissimilarity  
29 measures derived from  $N_{ST}$ ,  $G_{ST}$  and haplotypes. Thus, for these three measures it is plausible that  
30 regional signatures of East-West differentiation are confounded by alternative signatures, such as  
31 isolation by distance, present in other PBS.  
32  
33  
34  
35  
36  
37

38 The phylogeographic data support a general model where individual relatedness is described  
39 by topoclimatic variation, with the predominant structure being western and eastern populations. In  
40 total, eastern and western populations were inferred with nuclear genetic data for 13 of the 16 PBS  
41 analysed, of which five presented no regional mtDNA structure. Landscape variation for climate and  
42 topography explained geographic patterns of genomic relatedness within all 13. Twelve of these PBS  
43 presented signatures of admixture, which were concentrated around sites 5 and 6 for 11 PBS (Fig. 4).  
44  
45  
46  
47 This is strong evidence for a shared dynamic within a community-level model, the explanation of  
48 which requires an understanding of the geological history of the Anaga peninsula itself.  
49  
50  
51  
52  
53  
54  
55  
56  
57  
58  
59  
60



1  
2  
3  
4  
5  
6  
7  
8  
9  
10 Instability of the northern flank of Anaga, between sites 1 and 6 (Fig. 1), led to partial seaward  
11 collapse, estimated between 4.1 - 4.7 Ma (Walter *et al.* 2005) of approximately 15 km<sup>2</sup> of surface  
12 area (García-Olivares *et al.* 2017). A more than 4 million-year old topographic footprint of the Anaga  
13 mega-landslide is visible today as steep northern slopes and an approximately 115 m drop in elevation  
14 between sites 4 and 5 (Fig. 4). This saddle represents the lowest crestral elevation across the sampling  
15 area, and is likely to have been a consistent topographic feature of the region since the landslide  
16 happened (Fig. S2). Elevation itself is a proxy for an important source of moisture, not included in  
17 our model due to its local and idiosyncratic nature. A thermal inversion layer varies in elevation  
18 throughout the year, regulating the formation, intensity and frequency of stratocumulus clouds  
19 (Sperling *et al.* 2004). More intense and frequent cloud formation occurs at lower elevations (700-  
20 900 metres above current sea level; macsl) during the regionally dryer summer months (Marzol  
21 2008). With crest elevation dropping to as low as 675 macsl, the region between sites 4 and 5 falls  
22 below the cloud formation that maintains a humid environment from site 4 to the east and from site  
23 5 to the west through condensation (del Arco Aguilar *et al.* 2006; Braojos Ruiz 2015). This limited  
24 water capture from condensation further contributes to water stress within the generally dryer and  
25 warmer climate of the saddle region (Fig. S3).  
26  
27  
28  
29  
30  
31  
32  
33  
34  
35  
36

37 While the geographic distance between sites 4 and 5 (Fig. 1) measures only 3.7 km, our data  
38 clearly reveal that the dryer environmental conditions spanning this distance have been consequential  
39 for a large number of beetle species over the last several million years. Results are consistent with a  
40 model of geographic isolation by niche conservatism of climatic tolerance (Wiens & Graham 2005),  
41 in particular to humid conditions within the laurel forest, and facilitated by limited dispersal ability  
42 (flightlessness) for most species. While it is assumed that laurel forest beetle species are typically  
43 limited to this ecosystem (e.g. Fernández-Palacios *et al.* 2017), fundamental species distribution data  
44 is lacking. Using the limited species presence records that have been extrapolated from the literature,  
45 we applied the maximum entropy species distribution modelling approach (Maxent, Phillips *et al.*  
46 2006), providing results consistent with laurel forest affiliations for 13 of the 15 PBS (for details on  
47  
48  
49  
50  
51  
52  
53  
54  
55  
56  
57  
58  
59  
60

1  
2  
3  
4  
5  
6  
7  
8  
9  
10 methods and results, see Appendix S2). Two simple and contrasting mechanistic explanations can be  
11 put forward to explain the onset of East and West isolation within species, either: (i) colonisation  
12 from one region to the other by chance dispersal, or (ii) range vicariance driven by periods of  
13 suboptimal climate impacting species ranges (Fig. S4). Vicariance caused by the mega-landslide itself  
14 is a likely explanation for the early Pliocene divergence estimated within *Acalles globulipennis* (Table  
15 S1). However, all remaining PBS have divergence time estimates within the Quaternary, where both  
16 mechanisms may plausibly explain the origin of isolation. For all PBS, irrespective of the mechanism,  
17 divergence must also be reconciled with repeated inferences of secondary contact, concentrated  
18 around sites 5 and 6. In this context, cyclical altitudinal shifts in favourable environmental conditions  
19 are an expected consequence as Quaternary insular climate transitioned between glacial and  
20 interglacial conditions (Fernández-Palacios *et al.* 2016). The repeated evidence for coincident  
21 isolation and secondary contact presented here, together with mtDNA divergences ranging over the  
22 full extent of the Quaternary (Table S1), indicate a dynamic of isolation and secondary contact  
23 extending over multiple cycles of Quaternary climate oscillation. Recent climate models applied to  
24 laurel forest bryophytes (Patiño *et al.* 2016) predict that globally warmer interglacial conditions  
25 should result in higher water stress at lower elevations, and upslope shifts in range limits. Under such  
26 a model, regional isolation of hydrophilic beetles should be greatest during interglacial periods, such  
27 as now, with higher connectivity during cooler glacial conditions. However, an alternative model  
28 predicts reduced water stress at lower laurel forest elevations as climate transitions from glacial to  
29 interglacial conditions (Sperling *et al.* 2004), and it remains unclear which model best explains the  
30 spatiotemporal dynamics of the laurel forest. We suggest that these competing models, and their  
31 contrasting demographic predictions, could be directly tested with more detailed geographic sampling  
32 and genomic analysis of regionally structured species such as those presented here.

33  
34  
35  
36  
37  
38  
39  
40  
41  
42  
43  
44  
45  
46  
47  
48  
49 The importance of Quaternary climate oscillations for biodiversity distribution patterns  
50 among islands has recently been demonstrated (Rijsdijk *et al.* 2014; Weigelt *et al.* 2016). Our results  
51 extend this influence to within island diversification, revealing that subtle environmental  
52  
53  
54  
55  
56  
57  
58  
59  
60

1  
2  
3  
4  
5  
6  
7  
8  
9  
10 discontinuity over a limited geographic distance can structure genomic variation across multiple  
11 species. Although we do not suggest that population divergence will inevitably lead to speciation in  
12 all species, the potential for eventual speciation is demonstrated by *A. globulipennis*, where  
13 divergence between East and West populations is consistent with morphologically cryptic species  
14 (Hendrich *et al.* 2015; see Appendix S1), and exceeds divergences between related species within the  
15 subfamily Cryptorhynchini (Stüben & Astrin 2010). This strong and unprecedented support for a  
16 topoclimate-mediated, islands within islands model for speciation (García-Olivares *et al.* 2019) has  
17 important consequences for island biogeography, where it has previously been suggested that  
18 dispersal limitation and landscape variation may promote isolation and speciation within islands  
19 (Goodman *et al.* 2012), even at relatively small geographic scales (Vandergast *et al.* 2004).  
20 Topoclimatic mosaics should have been subjected to greater temporal stability during the Tertiary,  
21 enhancing isolation effects and the potential for speciation by reducing periodic opportunity for  
22 secondary contact. Thus, for taxa characterised by limitations to both dispersal ability and climatic  
23 tolerance, environmental discontinuities across topographically complex landscapes are likely to be  
24 a persistent driver of speciation throughout island ontogeny. More generally, our results suggest that  
25 topoclimatically variable continental landscapes may be important arenas for speciation, particularly  
26 when such landscapes were characterised by relative geological stability during the Tertiary, but were  
27 buffered from defaunation during Quaternary climatic oscillations. Finally, our results further  
28 highlight the sensitivity of arthropod species range limits to climate change (Robinet & Roques 2010).  
29 We suggest that when species dispersal ability and environmental tolerance are restricted,  
30 demographic impacts of climate change will be stronger, which may offer some explanation for  
31 recently reported variation in climate-related abundance declines for tropical arthropods (Lister &  
32 García 2018).

33  
34  
35  
36  
37  
38  
39  
40  
41  
42  
43  
44  
45  
46  
47  
48  
49 Isolated populations represent the incipient stages of speciation, and are thus of fundamental  
50 importance for understanding speciation (Mayr 1942). We have revealed repeated and coincident  
51 geographic isolation and genomic divergence within species across a spatially limited environmental  
52  
53  
54  
55  
56  
57  
58  
59  
60

1  
2  
3  
4  
5  
6  
7  
8  
9  
10 barrier, within a dynamic of divergence with gene flow. Divergence times within species range from  
11 less than 100 Ka to more than 4 Ma, providing different temporal snapshots of divergence along the  
12 speciation continuum within the same geographic setting. Our results highlight not only the  
13 importance of integrating ecological and evolutionary data to reveal process-based explanations for  
14 the generation and spatial structure of biodiversity, but also the fine spatial scale within which such  
15 processes can play out.  
16  
17  
18  
19  
20  
21  
22  
23  
24  
25  
26  
27  
28  
29  
30  
31  
32  
33  
34  
35  
36  
37  
38  
39  
40  
41  
42  
43  
44  
45  
46  
47  
48  
49  
50  
51  
52  
53  
54  
55  
56  
57  
58  
59  
60

For Review Only

## ACKNOWLEDGEMENTS

This research was supported by Spanish MINECO grants CGL2013-42589-P and CGL2017-85718-P, co-financed by FEDER and awarded to B.C.E, and by the ERA-Net Net-Biome research framework, financed through Canary Island Government ACIISI grants SE-12/04 and SE-12/02, co-financed by FEDER and awarded to P.O. and B.C.E respectively. A.S.-C. was funded by the Ministerio de Educación y Formación Profesional through the FPU PhD fellowship (FPU014/02948). J.P. was funded by the MINECO through the Juan de la Cierva Program - Incorporation (IJCI-2014-19691) and Ramón y Cajal Program (RYC-2016-20506), and Marie Skłodowska-Curie COFUND, Researchers' Night and Individual Fellowships Global (MSCA grant agreement No 747238, 'UNISLAND'). The authors wish to acknowledge the contribution of the Teide High-Performance Computing facility (TeideHPC) provided by the Instituto Tecnológico y de Energías Renovables (ITER), S.A, and to thank the following for assistance with field work and sample sorting: Rienk Apperloo, Manuel Arechavaleta, Salvador de la Cruz, Nuria Macías-Hernández, Benito Pérez Vispo, Sara Ravagni, Isa Sancibrián Span, and Nieves Zurita. We thank two anonymous reviewers for their insightful comments and useful suggestions.

## REFERENCES

- Ancochea, E., Fúster, J.M., Ibarrola, E., Cendrero, A., Hernan, F., Cantagrel, J.M. *et al.* (1990). Volcanic evolution of the island of Tenerife (Canary Islands) in the light of new K-Ar data. *Journal of Volcanology and Geothermal Research*, 44, 231-249.
- Baselga, A., Fujisawa, T., Crampton-Platt, A., Bergsten, J., Foster, P.G., Monaghan, M.T. *et al.* (2013). Whole-community DNA barcoding reveals a spatio-temporal continuum of biodiversity at species and genetic levels. *Nature Communications*, 4.
- Baselga, A. & Orme, C.D.L. (2012). betapart: an R package for the study of beta diversity. *Methods in Ecology and Evolution*, 3, 808-812.
- Bedward, M., Keith, D.A. & Pressey, R.L. (1992). Homogeneity analysis: Assessing the utility of classifications and maps of natural resources. *Austral Ecology*, 17, 133-139.
- Böhner, J. & Antonic, O. (2008). Land-surface parameters specific to topoclimatology. In: *Geomorphometry: Concepts, Software, Applications*. (eds. Hengl, T & Reuter, HI). Elsevier, pp. 195-226.
- Borregaard, M.K., Amorim, I.R., Borges, P.A.V., Cabral, J.S., Fernández-Palacios, J.M., Field, R. *et al.* (2017). Oceanic island biogeography through the lens of the general dynamic model: assessment and prospect. *Biological Reviews*, 92, 830-853.
- Bouckaert, R., Heled, J., Kühnert, D., Vaughan, T., Wu, C.-H., Xie, D. *et al.* (2014). BEAST 2: a software platform for Bayesian evolutionary analysis. *PLoS Computational Biology*, 10, e1003537.
- Braojos Ruiz, J.J. (2015). *La nube, el pino y la otra lluvia. Una metodología para evaluar el potencial de captación de agua de niebla y su aprovechamiento natural o artificial*. Consejo Insular de Aguas de Tenerife, Santa Cruz de Tenerife.
- Brown, R.P., Hoskisson, P.A., Welton, J.H. & Báez, M. (2006). Geological history and within-island diversity: a debris avalanche and the Tenerife lizard *Gallotia galloti*. *Molecular Ecology*, 15, 3631-3640.
- Cabral, J.S., Wiegand, K. & Kreft, H. (2019). Interractions between ecological, evolutionary, and environmental processes unveil complex dynamics of insular plant diversity. *Journal of Biogeography*, 46, 1582-1597.
- Carracedo, J.C. (2011). *Geología de Canarias I. Origen, evolución, edad y volcanismo*. Editorial Rueda, Madrid.
- Clarke, R.T., Rothery, P. & Raybould, A.F. (2002). Confidence limits for regression relationships between distance matrices: Estimating gene flow with distance. *Journal of Agriculture, Biological, and Environmental Statistics*, 7, 361-372.

- 1  
2  
3  
4  
5  
6  
7  
8  
9  
10 Conrad, O., Bechtel, B., Bock, M., Dietrich, H., Fischer, E., Gerlitz, L. *et al.* (2015). System for  
11 Automated Geoscientific Analyses (SAGA) v. 2.1.4. *Geoscientific Model Development*, 8,  
12 1991-2007.
- 13 Darriba, D., Taboada, G.L., Doallo, R. & Posada, D. (2012). jModelTest 2: more models, new  
14 heuristics and parallel computing. *Nature Methods*, 9, 772.
- 15 del Arco Aguilar, M.-J., Wildpret de la Torre, W., Pérez de la Paz, P.L., Rodríguez Delgado, O.,  
16 Acebes Ginovés, J.R., García Gallo, A. *et al.* (2006). *Mapa de vegetación de Canarias*.  
17 GRAFCAN, Santa Cruz de Tenerife.
- 18 Emerson, B.C., Casquet, J., López, H., Cardoso, P., Borges, P.A.V., Mollaret, N. *et al.* (2017). A  
19 combined field survey and molecular identification protocol for comparing forest arthropod  
20 biodiversity across spatial scales. *Molecular Ecology Resources*, 17, 694-707.
- 21 Emerson, B.C., Oromí, P. & Hewitt, G.M. (2000). Tracking colonisation and diversification of insect  
22 lineages on islands: MtDNA phylogeography of *Tarphius canariensis* (Coleoptera:  
23 Colydiidae) on the Canary Islands. *Proceedings of the Royal Society of London B*, 267, 2199-  
24 2205.
- 25 Fernández-Palacios, J.M., Arévalo, J.R., Balguerías, E., Barone, R., de Nascimento, L., Delgado, J.D.  
26 *et al.* (2017). *La Laurisilva. Canaria, Madeira y Azores*. Macaronesia Editorial, Santa Cruz  
27 de Tenerife.
- 28 Fernández-Palacios, J.M., Rijdsdijk, K.F., Norder, S.J., Otto, R., de Nascimento, L., Fernández-Lugo,  
29 S. *et al.* (2016). Toward a glacial-sensitive model of island biogeography. *Global Ecology*  
30 *and Biogeography*, 25, 817-830.
- 31 Frichot, E., François, O. & O'Meara, B. (2015). LEA: An R package for landscape and ecological  
32 association studies. *Methods in Ecology and Evolution*, 6, 925-929.
- 33 Frichot, E., Mathieu, F., Trouillon, T., Bouchard, G. & François, O. (2014). Fast and efficient  
34 estimation of individual ancestry coefficients. *Genetics*, 196, 973-983.
- 35 García-Olivares, V., López, H., Patiño, J., Alvarez, N., Machado, A., Carracedo, J.C. *et al.* (2017).  
36 Evidence for mega-landslides as drivers of island colonisation. *Journal of Biogeography*, 44,  
37 1053-1064.
- 38 García-Olivares, V., Patiño, J., Overcast, I., Salces-Castellano, A., López de Heredia, U., Mora-  
39 Márquez, F. *et al.* (2019). A topoclimate model for Quaternary insular speciation. *Journal of*  
40 *Biogeography*, in press.
- 41 Goodman, K.R., Welter, S.C. & Roderick, G.K. (2012). Genetic divergence is decoupled from  
42 ecological diversification in the Hawaiian *Nesosydne* planthoppers. *Evolution*, 66, 2798-2814.
- 43 Hardy, O.J. & Vekemans, X. (2002). SPAGeDi: a versatile computer program to analyse spatial  
44 genetic structure at the individual or population levels. *Molecular Ecology Notes*, 2, 618-620.
- 45  
46  
47  
48  
49  
50  
51  
52  
53  
54  
55  
56  
57  
58  
59  
60

- 1  
2  
3  
4  
5  
6  
7  
8  
9  
10 Hein, J., Schierup, M.H. & Wiuf, C. (2005). *Gene genealogies, variation and evolution*. Oxford  
11 University Press, New York.
- 12 Hendrich, L., Morinière, J., Haszprunar, G., Hebert, P.D.N., Hausman, A., Köhler, F. *et al.* (2015).  
13 A comprehensive DNA barcode database for Central European beetles with a focus on  
14 Germany: adding more than 3500 identified species to BOLD. *Molecular Ecology Resources*,  
15 15, 795-818.
- 16  
17 Ho, S.Y.W. & Duchêne, S. (2014). Molecular-clock methods for estimating evolutionary rates and  
18 timescales. *Molecular Ecology*, 23, 5947-5965.
- 19  
20 Huson, D.H. & Bryant, D. (2006). Application of phylogenetic networks in evolutionary studies.  
21 *Molecular Biology and Evolution*, 23, 254-267.
- 22  
23 Jombart, T. & Ahmed, I. (2011). adegenet 1.3-1: new tools for the analysis of genome-wide SNP  
24 data. *Bioinformatics*, 27, 3070-3071.
- 25  
26 Karger, D.N., Conrad, O., Böhrer, J., Kawohl, T., Kerft, H., Soria-Auza, R.W. *et al.* (2017).  
27 Climatologies at high resolution for the earth's land surface areas. *Scientific Data*, 4, 170122.
- 28  
29 Kisel, Y. & Barraclough, T.G. (2010). Speciation has a spatial scale that depends in levels of gene  
30 flow. *The American Naturalist*, 175, 316-334.
- 31  
32 Kivimäki, I., Shimbo, M. & Saerens, M. (2014). Developments in the theory of randomized shortest  
33 paths with a comparison of graph node distances. *Physica A: Statistical Mechanics and its  
34 Applications* 393, 600-616.
- 35  
36 Lim, J.Y. & Marshall, C.R. (2017). The true tempo of evolutionary radiation and decline revealed on  
37 the Hawaiian archipelago. *Nature*, 543, 710-713.
- 38  
39 Lister, B.C. & Garcia, A. (2018). Climate-driven declines in arthropod abundance restructure a  
40 rainforest food web. *Proceedings of the National Academy of Sciences of the United States of  
41 America*, 115, E10397-E10406.
- 42  
43 Losos, J.B. & Ricklefs, R.E. (2009). Adaptation and diversification on islands. *Nature*, 457, 830-836.
- 44  
45 Machado, A., Rodríguez-Expósito, E., López, M. & Hernández, M. (2017). Phylogenetic analysis of  
46 the genus *Laparocerus*, with comments on colonisation and diversification in Macaronesia  
47 (Coleoptera, Curculionidae, Entiminae). *Zookeys*, 651, 1-77.
- 48  
49 Manolopoulou, I., Legarreta, L., Emerson, B.C., Brooks, S.D. & Tavaré, S. (2011). A Bayesian  
50 approach to phylogeographic clustering. *Interface Focus*, 1, 909-921.
- 51  
52 Marzol, V.M. (2008). Temporal characteristics and fog water collection during summer in Tenerife  
53 (Canary Islands, Spain). *Atmospheric Research*, 87, 352-361.
- 54  
55 Mayr, E. (1942). *Systematics and the origin of species from the viewpoint of a zoologist*. Harvard  
56 University Press, Cambridge, Massachusetts.  
57  
58  
59  
60



- 1  
2  
3  
4  
5  
6  
7  
8  
9  
10 McRae, B.H., Dickson, B.G., Keitt, T.H. & Shah, V.B. (2008). Using circuit theory to model  
11 connectivity in ecology, evolution, and conservation. *Ecology*, 89, 2712-2724.
- 12 McRae, B.H. & Shah, V.B. (2009). Circuitscape user's guide. Available at: [www.circuitscape.org](http://www.circuitscape.org).
- 13 Murtagh, F. & Legendre, P. (2014). Ward's Hierarchical Agglomerative Clustering Method: Which  
14 Algorithms Implement Ward's Criterion? *Journal of Classification*, 31, 274-295.
- 15 Papadopoulou, A., Anastasiou, I. & Vogler, A.P. (2010). Revisiting the insect mitochondrial  
16 molecular clock: the mid-Aegean trench calibration. *Molecular Biology and Evolution*, 27,  
17 1659-1672.
- 18 Patiño, J., Mateo, R.G., Zanatta, F., Marquet, A., Aranda, S.C., Borges, P.A.V. *et al.* (2016). Climate  
19 threat on the macaronesian endemic bryophyte flora. *Scientific Reports*, 6, 29156.
- 20 Peterman, W.E. (2018). ResistanceGA: An R package for the optimisation of resistance surfaces  
21 using genetic algorithms. *Methods in Ecology and Evolution*, 9, 1638-1647.
- 22 Peterman, W.E., Connette, G.M., Keitt, T.H. & Shah, V.B. (2014). Ecological resistance surfaces  
23 predict fine-scale genetic differentiation in a terrestrial woodland salamander. *Molecular  
24 Ecology*, 23, 2402-2413.
- 25 Petkova, D., Novembre, J. & Stephens, M. (2015). Visualising spatial population structure with  
26 estimated effective migration surfaces. *Nature Genetics*, 48, 94-100.
- 27 Phillips, S.J., Anderson, R.P. & Schapire, R.E. (2006). Maximum entropy modeling of species  
28 geographic distributions. *Ecological Modelling*, 190, 231-259.
- 29 Rijdsdijk, K.F., Hengl, T., Norder, S.J., Otto, R., Emerson, B.C., Ávila, S.P. *et al.* (2014). Quantifying  
30 surface-area changes of volcanic islands driven by Pleistocene sea-level cycles:  
31 biogeographical implications for the Macaronesian archipelagos. *Journal of Biogeography*,  
32 41, 1242-1254.
- 33 Robinet, C. & Roques, A. (2010). Direct impacts of recent climate warming on insect populations.  
34 *Integrative Zoology*, 5, 132-142.
- 35 Robinson, N., Regetz, J. & Guralnick, R.P. (2014). EarthEnv-DEM90: A nearly-global, void-free,  
36 multi-scale smoothed, 90m digital elevation model from fused ASTER and SRTM data.  
37 *ISPRS Journal of Photogrammetry and Remote Sensing*, 87, 57-67.
- 38 Rominger, A.J., Goodman, K.R., Lim, J.Y., Armstrong, E.E., Becking, L.E., Bennett, G.M. *et al.*  
39 (2016). Community assembly on isolated islands: macroecology meets evolution. *Global  
40 Ecology and Biogeography*, 25, 769-780.
- 41 Rosindell, J. & Harmon, L.J. (2013). A unified model of species immigration, extinction and  
42 abundance on islands. *Journal of Biogeography*, 40, 1107-1118.
- 43  
44  
45  
46  
47  
48  
49  
50  
51  
52  
53  
54  
55  
56  
57  
58  
59  
60

Field Code Changed

- 1  
2  
3  
4  
5  
6  
7  
8  
9  
10 Schütte, A. & Stüben, P.E. (2015). Molecular systematics and morphological identification of the  
11 cryptic species of the genus *Acalles* Schoenherr, 1825, with descriptions of new species  
12 (Coleoptera: Curculionidae: Cryptorhynchinae). *Zootaxa*, 3945, 001-051.
- 13 Shaw, K.L. & Gillespie, R.G. (2016). Comparative phylogeography of oceanic archipelagos:  
14 Hotspots for inferences of evolutionary process. *Proceedings of the National Academy of*  
15 *Sciences of the United States of America*, 113, 7986-7993.
- 16 Sperling, F.N., Washington, R. & Whittaker, R.J. (2004). Future climate change of the subtropical  
17 North Atlantic: implications for the cloud forests of Tenerife. *Climate Change*, 65, 103-123.
- 18 Stüben, P.E. & Astrin, J.J. (2010). Molecular phylogeny in endemic weevils: revision of the genera  
19 of Macaronesian Cryptorhynchinae (Coleoptera: Curculionidae). *Zoological Journal of the*  
20 *Linnean Society*, 40-87.
- 21 Thirlwall, M.F., Singer, B.S. & Marriner, G.F. (2000). <sup>39</sup>Ar-<sup>40</sup>Ar ages and geochemistry of the  
22 basaltic shield stage of Tenerife, Canary Islands, Spain. *Journal of Volcanology and*  
23 *Geothermal Research*, 103, 247-297.
- 24 van Etten, J.R. (2017). R Package gdistance: Distances and Routes on Geographical Grids. *Journal*  
25 *of Statistical Software*, 76.
- 26 Vandergast, A.G., Gillespie, R.G. & Roderick, G.K. (2004). Influence of volcanic activity on the  
27 population genetic structure of Hawaiian *Tetragnatha* spiders: fragmentation, rapid  
28 population growth and the potential for accelerated evolution. *Molecular Ecology*, 13, 1729-  
29 1743.
- 30 Walter, T.R., Troll, V.R., Cailleau, B., Belousov, A., Schmincke, H.-U., Amelung, F. *et al.* (2005).  
31 Rift zone reorganisation through flank instability in ocean island volcanoes: an example from  
32 Tenerife, Canary Islands. *Bulletin of Volcanology*, 67, 281-291.
- 33 Weigelt, P., Steinbauer, M.J., Cabral, J.S. & Krefft, H. (2016). Late Quaternary climate change shapes  
34 island biodiversity. *Nature*, 532, 99-102.
- 35 Whittaker, R.J., Triantis, K.A. & Ladle, R.J. (2008). A general dynamic theory of oceanic island  
36 biogeography. *Journal of Biogeography*, 35, 977-994.
- 37 Wiens, J.J. & Graham, C.H. (2005). Niche conservatism: Integrating Evolution, Ecology, and  
38 Conservation Biology. *Annual Review of Ecology, Evolution and Systematics*, 36.
- 39  
40  
41  
42  
43  
44  
45  
46  
47  
48  
49  
50  
51  
52  
53  
54  
55  
56  
57  
58  
59  
60

1  
2  
3  
4  
5  
6  
7  
8  
9  
10  
11  
12  
13  
14  
15  
16  
17  
18  
19  
20  
21  
22  
23  
24  
25  
26  
27  
28  
29  
30  
31  
32  
33  
34  
35  
36  
37  
38  
39  
40  
41  
42  
43  
44  
45  
46  
47  
48  
49  
50  
51  
52  
53  
54  
55  
56  
57  
58  
59  
60

**Competing interests.** The authors declare no competing interests.

**Code availability.** The R script for the delimitation of presumed biological species is available from GitHub: [https://github.com/\[to be made available upon acceptance\]](https://github.com/[to be made available upon acceptance]).

For Review Only

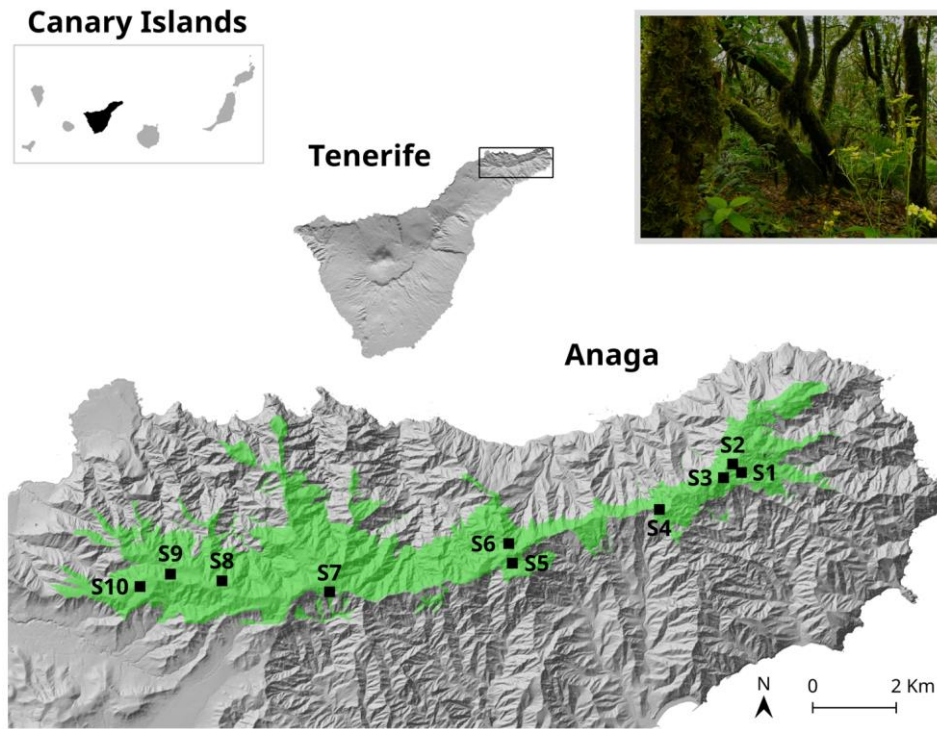


**Figure 1** Sampling plots within the laurel forest of the Anaga peninsula of Tenerife, Canary Islands. The ten sampling plots are labelled, from east to west, S1 - S10, and the potential extent of the laurel forest within the Anaga peninsula (del Arco Aguilar *et al.* 2006) is shown in green. Top right inset shows typical laurel forest vegetation.

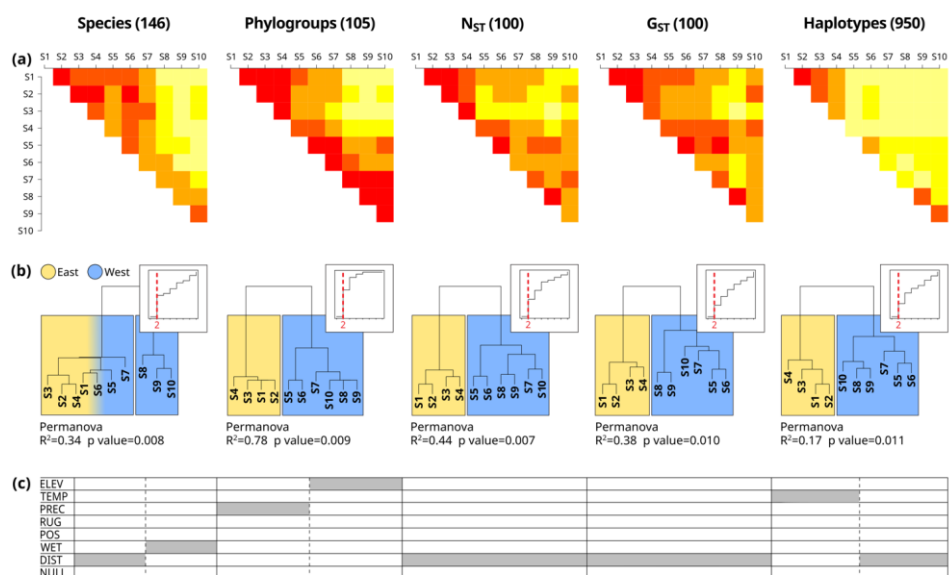


**Figure 2** Patterns of community similarity among sampling plots. (a) Dissimilarity matrices among the ten sampling plots are presented at the level of presumed biological species (PBS) and four different treatments of intraspecific genetic variation: phylogroups, average  $N_{ST}$  and  $G_{ST}$  across all PBS, and all haplotypes across all PBS, where red represents maximum similarity between plots and light yellow represents maximum dissimilarity. Numbers in brackets correspond to the number of PBS sampled for each analysis, with the exception of haplotypes, where it represents the total number of haplotypes analysed. Sampling sites S1-S10 correspond to Fig. 1. (b) Hierarchical cluster analyses of dissimilarity matrices in A, with inset showing the increase in the average within-group pairwise similarity (y axis = homogeneity) across the different number of groups of plots defined by the hierarchical classification (x axis). Repeated clustering of the four eastern and six western plots for the four treatments of intraspecific genetic variation, together with maximum increase in homogeneity, is highlighted with yellow and blue colours respectively. Significant differences

1  
2  
3  
4  
5  
6  
7  
8  
9  
10 between the four eastern vs the six western plots defined for each of the four dissimilarity matrices  
11 of intraspecific genetic variation were revealed by Permanova analyses. (c) Landscape resistance  
12 analyses showing optimal models (indicated with shading, separated by a dashed line when there is  
13 more than one optimal model) that explain genetic structure within each of the dissimilarity matrices  
14 in A. ELEV = elevation, TEMP = temperature, PREC = precipitation, RUG = topographic rugosity,  
15 POS = topographic position index, WET = topographic wetness index, DIST = Euclidean distance,  
16 NULL = null model. See Table S3 for specific details.  
17  
18  
19  
20  
21  
22  
23  
24  
25  
26  
27  
28  
29  
30  
31  
32  
33  
34  
35  
36  
37  
38  
39  
40  
41  
42  
43  
44  
45  
46  
47  
48  
49  
50  
51  
52  
53  
54  
55  
56  
57  
58  
59  
60

For Review Only

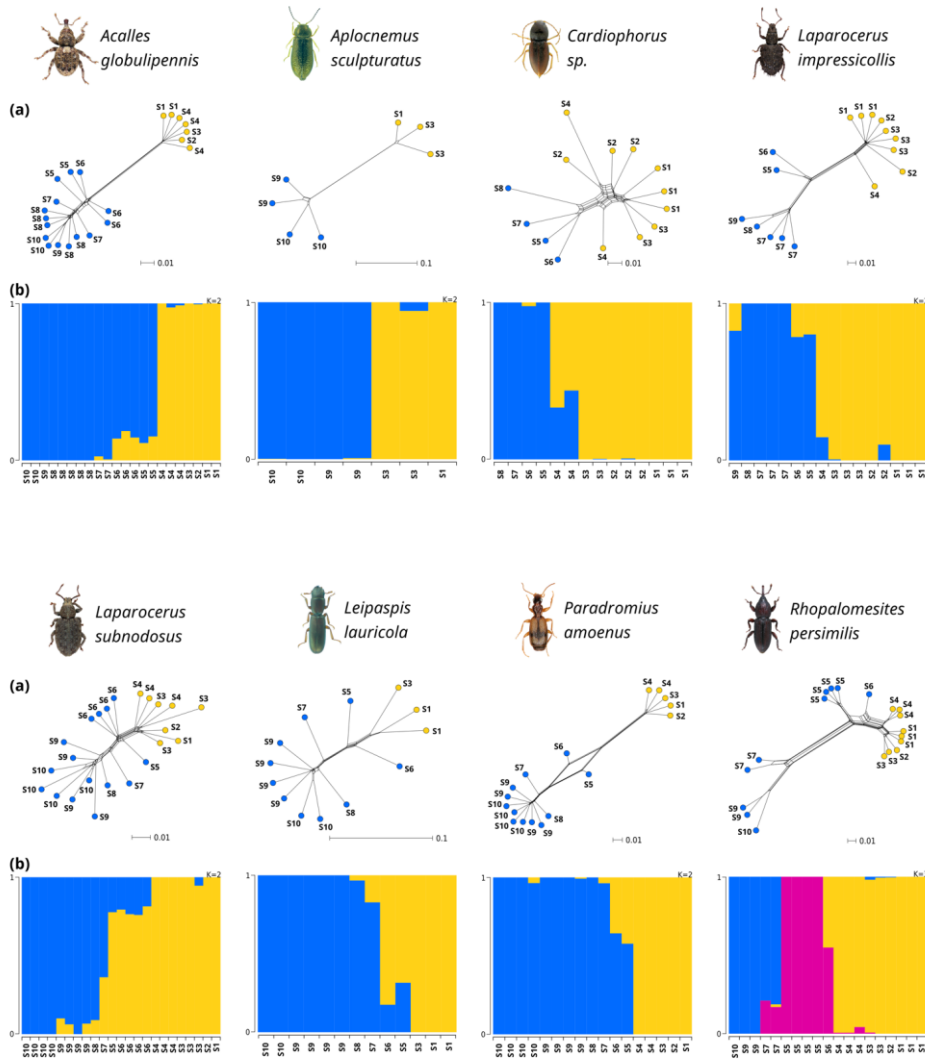


**Figure 3** Regional structuring of beetle genetic variation across the Anaga peninsula of Tenerife. Based on East-West regional patterns of mtDNA structure, ddRAD-seq data was generated for eight PBS (Table S1). (a) Haplotype networks constructed with ddRAD-seq data using the NeighborNet method in SplitsTree. The four eastern and six western plots are highlighted with yellow and blue

1  
2  
3  
4  
5  
6  
7  
8  
9  
10 colours, respectively, and codes correspond to sampling locations presented in Fig. 1. Each circle  
11 represents an individual, scale bars represent the proportion of inferred mutational change along  
12 branches. (b) Ancestry estimation matrices from model-based clustering analyses, using ddRAD-  
13 seq data. When optimal K (number of inferred ancestral populations) was inferred to be two or three,  
14 this is indicated with K=2 or K=3 respectively. K was forced to two for *Cardiophorus* sp. and  
15 *Leipaspis lauricola*, where optimal K was inferred to be one, to test the specific hypothesis of  
16 regional structuring between eastern and western populations. Blue and yellow represent proportion  
17 of genomic assignment to eastern and western ancestry respectively. In the case of *R. persimilis*, a  
18 third (central) ancestral population is represented in pink. See Fig. S1 for mtDNA haplotype  
19 networks and ddRAD-seq PCA plots for each PBS, and all results for eight PBS with no regional  
20 structuring of mtDNA.  
21  
22  
23  
24  
25  
26  
27  
28  
29  
30  
31  
32  
33  
34  
35  
36  
37  
38  
39  
40  
41  
42  
43  
44  
45  
46  
47  
48  
49  
50  
51  
52  
53  
54  
55  
56  
57  
58  
59  
60



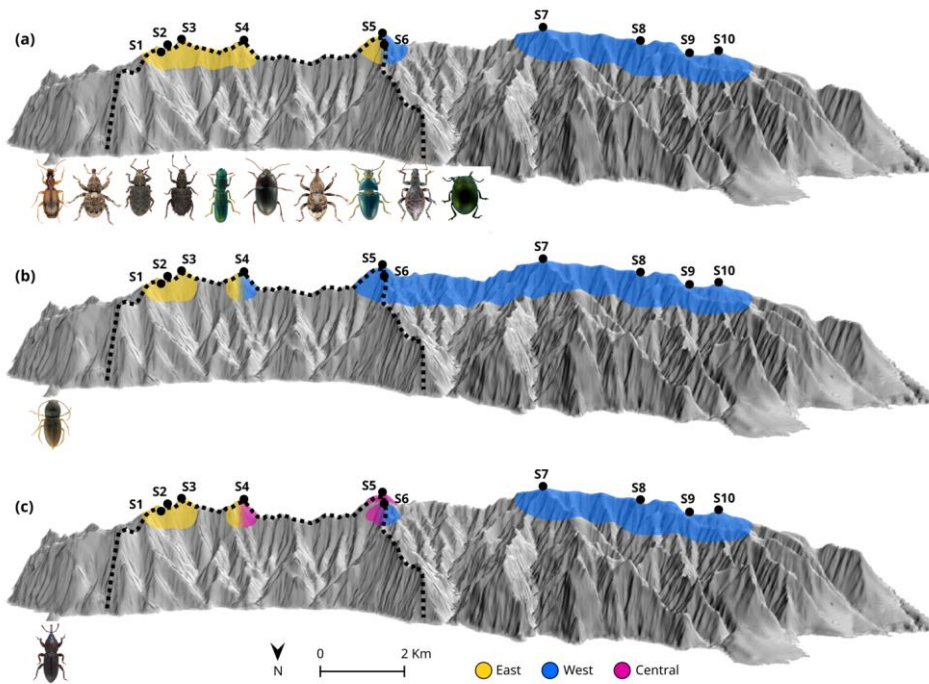


**Figure 4** Repeated regional structuring of beetle intraspecific nuclear genomic variation across the Anaga peninsula. The Anaga peninsula is shown looking down onto its northern flank, with sampling sites labelled as in Fig. 1. Broken black lines denote the limits of a mega-landslide estimated to have occurred between 4.1 - 4.7 Ma (Walter *et al.* 2005). Different ancestral populations inferred from individual ancestry coefficients estimated with the program sNMF (see Methods) are represented with different colours. Twelve of sixteen species of beetle analysed with ddRAD-seq data (see Fig. S1) present evidence for regional structuring of inferred ancestral gene pools with geographically intermediate admixture, each fitting one of three models: (a) eastern (yellow) and western (blue) populations and admixed genomes centred around S5 and S6. This model is observed for the ten

1  
2  
3  
4  
5  
6  
7  
8  
9  
10 species pictured, from left to right, *Paradromius amoenus*, *Acalles globulipennis*, *Laparocerus*  
11 *subnodosus*, *Laparocerus impressicollis*, *Leipaspis lauricola*, *Amaroschema gaudini*, *Silvacalles*  
12 *instabilis*, *Xestus throscoides*, *Laparocerus ellipticus* and *Chrysolina costalis*; (b) *Cardiophorus* sp.  
13  
14 (pictured) is separated into eastern (yellow) and western (blue) populations, distributed either side of  
15 admixed genomes in S4; (c) *Rhopalomesites persimilis* (pictured) is separated into eastern (yellow),  
16 central (pink) and western (blue) populations, with admixed genomes in geographically intermediate  
17 plots between east and central (S4) and central and west (S6).  
18  
19  
20  
21  
22  
23  
24  
25  
26  
27  
28  
29  
30  
31  
32  
33  
34  
35  
36  
37  
38  
39  
40  
41  
42  
43  
44  
45  
46  
47  
48  
49  
50  
51  
52  
53  
54  
55  
56  
57  
58  
59  
60